The extraordinary role of the AlN interlayer in growth of AlN sputtered on Ti electrodes

A. T. Tran, G. Pandraud, F. D. Tichelaar, M. D. Nguyen, H. Schellevis, and P. M. Sarro

---

The extraordinary role of the AlN interlayer in growth of AlN sputtered on Ti electrodes

A. T. Tran,[1,a)] G. Pandraud,[1] F. D. Tichelaar,[2] M. D. Nguyen,[3] H. Schellevis,[1] and P. M. Sarro[1]

[1]*Laboratory of Electronic Components, Technology, and Materials (ECTM), DIMES, Delft University of Technology, P.O. Box 5053, 2600 GB Delft, The Netherlands*
[2]*Kavli Institute of Nanoscience, Faculty of Applied Sciences, Delft University of Technology, 2628 CJ, Delft, The Netherlands*
[3]*MESA+ Institute for Nanotechnology, University of Twente, P.O. Box 217, 7500AE Enschede, The Netherlands*

The structure of AlN layers grown on Ti with and without an AlN interlayer between the Si substrate and the Ti layer is investigated. The AlN grains take over the orientation of the Ti columnar grains in both cases. Surprisingly, the Ti grains do not take over completely the orientations of the AlN grains of the interlayer, and show the same columnar grain structure as the sample without interlayer. Hence, the structure of the AlN top layer is independent of the presence of an AlN interlayer below the Ti layer and is mainly determined by the Ti layer microstructure. © 2013 AIP Publishing LLC. [http://dx.doi.org/10.1063/1.4835035]

The growth of aluminum nitride (AlN) thin film on a metal electrode has been widely studied because of its potential application in many devices, such as piezoelectric resonators,[1,2] nanoelectromechanical actuators,[3] and energy harvesting devices.[4] The piezoelectric properties of AlN strongly depend on the crystallinity,[5] c-axis orientation,[6] and polar distribution of the film structure.[7] Up to now, the very good crystalline structure was obtained by sputtering AlN films on Platinum (Pt) substrates.[8] Alternatively, Molybdenum (Mo) has also been investigated,[8] but both Pt and Mo are not CMOS compatible. Further, the difficulty in patterning those metals accurately and the poor adhesion to Si substrate strongly limits the applicability of these layers. Recently, Ti electrodes have been investigated as an alternative for CMOS compatibility.[9] However, a lower quality of the AlN layers has been reported in comparison to AlN deposited on Pt.[9,10] By using an AlN interlayer below the Ti an improved crystallinity and orientation of the AlN layers has been observed.[9,10] This is attributed to the decrease of the crystallization energy of the electrodes possibly caused by the AlN interlayer.[10,11] Recently, we reported on the use of this interlayer as a stop layer when releasing MEMS piezoelectric actuators.[12]

Here, we look into the influence of an AlN interlayer on the AlN top layer sputtered on Ti electrodes, focusing on the role of the interface between AlN and Ti. The obtained results suggest a different phenomenon and mechanism of the AlN growth on Ti electrode as previously reported.[10,11]

AlN films and Ti electrodes were deposited on (100) Si substrates in a DC magnetron sputtering setup (Sigma 204DC magnetron PVD system) in a similar way as described in Refs. 13 and 14. To avoid oxidation and possible contamination of the interface, Ti and AlN were sequentially sputtered without breaking the vacuum. The thicknesses of the top AlN thin film, the Ti electrode and the bottom AlN interlayer were

460 nm, 170 nm, and 100 nm, respectively. The layers were characterized using x-ray diffraction (XRD) (Philips XPERT-MPD D5000) and high resolution transmission electron microscopy (HR-TEM) (FEI Tecnai F20ST/STEM) to understand the role of the interlayer and the interface relationship between the AlN and the Ti electrode on the AlN crystallinity. All TEM images were obtained with the electron beam parallel to the Si substrate surface, facing the Si $\langle 110 \rangle$ orientation.

The θ-2θ XRD profiles of these samples with the appearance of only (002) and (004) hexagonal AlN reflections indicate highly c-axis orientated films.[12,14] Figure 1 shows the (002) peak x-ray rocking curve measurements of AlN/Si(100), AlN/Ti/Si(100), and AlN/Ti/AlN/Si(100) samples with the same 460 nm thickness of the AlN top layer. The decrease of FWHM of x-ray rocking curve from 3.0° for AlN/Si, to 1.3° for AlN/Ti/Si and 1.4° for AlN/Ti/AlN/Si (Ref. 14) indicates the great improvement of the AlN microstructures in the AlN/Ti/Si and AlN/Ti/AlN/Si samples, compared to AlN on bare Si. This
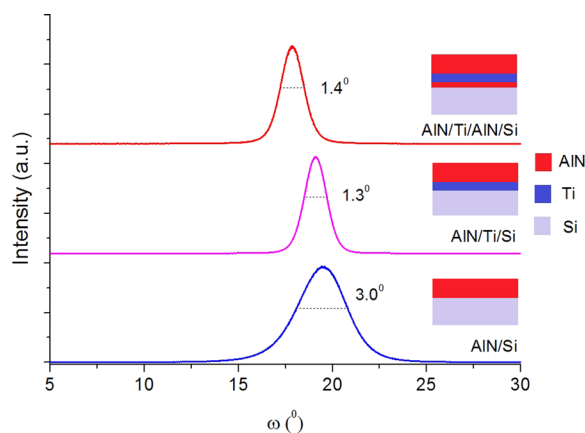
FIG. 1. The (002) peak the x-ray rocking curve measurements of AlN thin films deposited on different substrates: AlN/Si, AlN/Ti/Si, and AlN/Ti/AlN/Si.

a)Electronic mail: an.tran@tudelft.nl
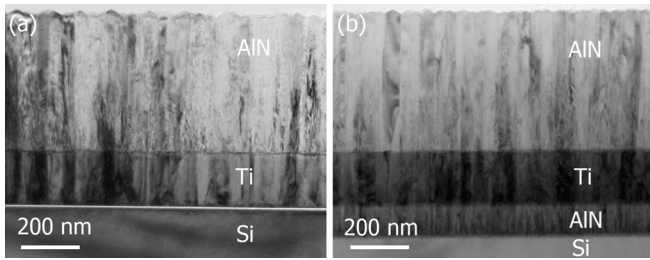
FIG. 2. BF TEM images of (a) AlN/Ti/Si and (b) AlN/Ti/AlN/Si samples.

observation is not in line with results previously published for similar structures [AlN/Ti/Si vs AlN/Ti/AlN/Si (Ref. 10) and AlN/Mo/AlN/Si vs AlN/Mo/AlN/Si (Ref. 11)]. In our case, the high crystallinity of the AlN on Ti indicated by rocking curve measurements is similar with or without the AlN interlayer.

A detailed analysis of the structures of the AlN/Ti/Si and AlN /Ti/AlN/Si samples was carried out by bright field (BF) TEM (Figures 2(a) and 2(b)). These results also show that the AlN interlayer grown on bare Si (100) consists of 10-20 nm wide columnar grains (Figure 2(a)). Furthermore, the top AlN layers in both cases contain the fiber texture columnar structure with an average grain width of ∼36 nm. These results are consistent with the XRD measurements reported above. All of the AlN and Ti grains have {0001} planes parallel to the substrate. The Ti {0001} crystal planes grow continuously on the AlN crystals.

In the AlN/Ti/Si sample, AlN and Ti have the same columnar structure. The Ti electrode layer in the AlN/Ti/AlN/Si sample presents grains that partly take over the orientation of the AlN interlayer. In Figure 2(b), we see that many grains continuously grow from the AlN interlayer through the Ti into the upper AlN layer. However, the Ti and upper AlN layer grains are clearly wider than the underlying AlN grains. This is in contrast to what is observed for AlN grown on Mo with an AlN interlayer as reported in Ref. 11, where the layers have the same columnar size. The higher quality of the upper AlN layer observed in our case mostly depends on the growth of the Ti bottom electrode grains. In our experiments the crystallinity of the Ti layer is mainly influenced by sputtering parameters and not the substrate (Silicon or AlN). This means that the AlN interlayer has a minor role on the crystallization of Ti layer. Furthermore, we found that the grain size of the AlN films on a Ti electrode directly takes over the grain size present at the surface of the
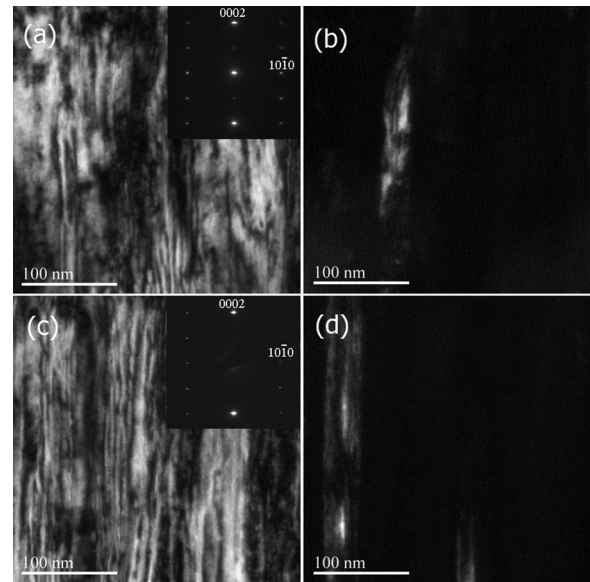
FIG. 4. DF TEM images using the reflections indicated in the diffraction patterns: (0002) reflections in (a) and (c), and ($10\bar{1}0$) reflections in (b) and (d). The cross-sectional images (a) and (b) were taken from the same area in the AlN/Ti/Si sample, (c) and (d) from the same area in the AlN/Ti/AlN/Si sample. The electron beam direction was a [110] direction in the Si substrate. A beam stopper was used for the diffraction pattern in (c).

Ti layer. HR-TEM together with Selected Area Diffraction Pattern (SADP) at the interface of AlN and Ti shown in Figure 3 indicate the local epitaxial growth even for high surface roughness at the interfaces (∼7 nm at Ti/AlN in AlN/Ti/Si sample and ∼10 nm at Ti/ AlN on AlN /Ti/AlN/Si sample). This means that local epitaxial growth of AlN on Ti is still preserved despite the rougher surface of the Ti layer, caused by the presence of the AlN interlayer. A similar observation applies also to the interface of Ti and AlN interlayer with lower surface roughness (∼4 nm) as indicated in the HR-TEM image (Figure 3(c)). We observe that the samples show a strong ⟨0002⟩ fiber texture both in the Ti and in the AlN layers. Hence, all diffraction patterns obtained with the electron beam direction parallel to the surface of the substrate, show strong {0002} reflections. Other reflections depend on the orientation of the crystals included in the selected area for diffraction. The HR-TEM images also confirm that the {0001} planes in AlN and Ti are both parallel to the substrate, which is in agreement with XRD measurements. Based on these findings, we can conclude that the enhancement of AlN crystals was not related to the AlN
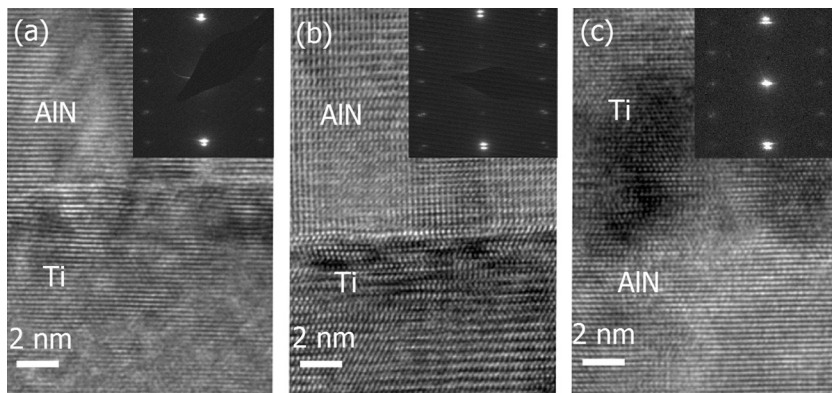
FIG. 3. HR-TEM and SADP images at the interface of the top AlN and the Ti electrode in the AlN/Ti/Si sample (Fig. 3(a)) and the AlN/Ti/AlN/Si sample (Fig. 3(b)); (c) the HR-TEM SADP images at the interface of the Ti electrode and AlN interlayer. The SADP images show in the vertical direction the {0002} reflections of Ti and of AlN (AlN reflections closer to the origin). In SADP images of Figs. 3(a) and 3(b), the central beam (origin) is blocked with a beam stopper.

interlayer as mentioned in Refs. 10 and 11 but is caused by the continuous growth of the AlN on Ti crystals, which have a larger width than the AlN underlayer (grown directly on Si).

Further investigation of the top AlN layer in AlN/Ti/Si and AlN/Ti/AlN/Si samples is revealed in the dark-field (DF) TEM images and diffraction patterns in Figure 4. In the DF images of both samples, taken with the common (0002) reflection in the textured layers in Figures 4(a) and 4(c), almost all grains light up. In contrast, when imaged with the uncommon (10$\bar{1}$0) reflection, only a few grains light up, as shown in the DF images in Figures 4(b) and 4(d).

In all DF images in Figure 4, intensity variations within a grain are caused by vertical dislocations, recognized by the narrow lines, and also by bending of the thin TEM foil. The DF images show a very similar structure of the top AlN layers in both samples with and without AlN interlayer below the Ti.

In summary, we observed a continuous growth of AlN on Ti such that the Ti grain width determines the AlN grain width on top. Particularly, the Ti grain structure was found to be independent on the presence or absence of an AlN interlayer. The Ti grains are much wider than those in the AlN interlayer and are similar to the grains of the Ti grown directly on the Si substrate. The similar {0002} textures of the grains of Ti on AlN and AlN on Ti have been clearly demonstrated.

[1] A. D. O'Connell, M. Hofheinz, M. Ansmann, R. C. Bialczak, M. Lenander, E. Lucero, M. Neeley, D. Sank, H. Wang, M. Weides, J. Wenner, J. M. Martinis, and A. N. Cleland, Nature **464**, 697 (2010).

[2] R. B. Karabalin, M. H. Matheny, X. L. Feng, E. Defay, G. Le Rhun, C. Marcoux, S. Hentz, P. Andreucci, and M. L. Roukes, Appl. Phys. Lett. **95**, 103111 (2009).

[3] N. Sinha, G. E. Wabiszewski, R. Mahameed, V. V. Felmetsger, S. M. Tanner, R. W. Carpick, and G. Piazza, Appl. Phys. Lett. **95**, 053106 (2009).

[4] A. Massaro, S. De Guido, I. Ingrosso, R. Cingolani, M. De Vittorio, M. Cori, A. Bertacchini, L. Larcher, and A. Passaseo, Appl. Phys. Lett. **98**, 053502 (2011).

[5] H. P. Loebl, M. Klee, C. Metzmacher, W. Brand, R. Milsom, and P. Lok, Mater. Chem. Phys. **79**(2–3), 143 (2003).

[6] A. Sanz-Hervas, M. Clement, E. Iborra, L. Vergara, J. Olivares, and J. Sangrador, Appl. Phys. Lett. **88**, 161915 (2006).

[7] M. Akiyama, T. Kamohara, N. Ueno, M. Sakamoto, K. Kano, A. Teshigahara, and N. Kawahara, Appl. Phys. Lett. **90**, 151910 (2007); T. Kamohara, M. Akiyama, and N. Kuwano, *ibid.* **92**, 093506 (2008); T. Kamohara, M. Akiyama, N. Ueno, M. Sakamoto, K. Kano, A. Teshigahara, N. Kawahara, and N. Kuwano, *ibid.* **89**, 243507 (2006).

[8] R. Lanz and P. Muralt, IEEE Trans. Ultrason. Ferroelectr. Freq. Control **52**, 936 (2005).

[9] J. C. Doll, B. C. Petzold, B. Ninan, R. Mullapudi, and B. L. Pruitt, J. Micromech. Microeng. **20**, 025008 (2010).

[10] T. Kamohara, M. Akiyama, N. Ueno, K. Nonaka, and N. Kuwano, Thin Solid Films **515**, 4565 (2007).

[11] T. Kamohara, M. Akiyama, N. Ueno, K. Nonaka, and N. Kuwano, Appl. Phys. Lett. **89**, 071919 (2006).

[12] A. T. Tran, G. Pandraud, H. Schellevis, T. Alan, V. Aravindh, O. Wunnicke, and P. M. Sarro, in *Procedia Engineering 25 (2011): Proceedings of Eurosensors XXV, Athens, Greece, 4-7 September 2011*, edited by G. Kaltsas and C. Tsamis (Elsevier Ltd., 2011), pp. 673–676.

[13] A. T. Tran, H. Schellevis, H. T. M. Pham, C. Shen, and P. M. Sarro in *Procedia Engineering 5 (2010): Proceedings of Eurosensors XXIV, Linz, Austria, 5-8 September 2010*, edited by B. Jakoby and M. J. Vellekoop (Elsevier Ltd., 2010), pp. 886–889.

[14] A. T. Tran, O. Wunnicke, G. Pandraud, M. D. Nguyen, H. Schellevis, and P. M. Sarro, Sens. Actuators, A **202**, 118 (2013).